Environ Monit Assess (2024) 196:1190
https://doi.org/10.1007/s10661-024-13363-x

RESEARCH

Evaluating the impact of climate change on yield and water use efficiency of different dry-season rice varieties cultivated under conventional and alternate wetting and drying conditions

Chan Arun Phoeurn · Aurore Degré · Chantha Oeurng · Pinnara Ket

Received: 7 May 2024 / Accepted: 29 October 2024

Abstract This study is the first attempt to assess rice cultivation under alternate wetting and drying (AWD) and continuous flooding (CF) using the latest scenarios from the Intergovernmental Panel on Climate Change (IPCC), utilizing AquaCrop Model. Field experiments were conducted during the dry season 2023 to get the model calibration and validation input. We used two shared socioeconomic pathways scenarios (SSP3-7.0 and SSP5-8.5) developed within Coupled Model Intercomparison Project Phase 6 (CMIP6) and projected the rice growth during 2040–2070. The simulation results demonstrated the effectiveness of AquaCrop in capturing crop development across treatments and varieties. This model's accuracy in simulating canopy cover (nRMSE = 14–32.5%), time series biomass (nRMSE = 22–42.5%), grain yield (Pd = 4.36–24.38%), and total biomass (nRMSE = 0.39–18.98%) was generally acceptable. The analysis of future climate shows an increasing trend in the monthly average temperature by 0.8 °C (Tmin) and 1.3 °C (Tmax) in both scenarios. While ETo values were not anticipated, rainfall was expected to increase with average values of 5.62 mm to 11.25 mm. In addition, the study found that varieties with growing periods longer than 93 days after transplanting (DAT), such as CAR15 and Sen Kra Ob, were most impacted by heat stress conditions, leading to reduced yield, harvest index (HI), and water use efficiency (WUE). In our case, CAR15 and Sen Kra Ob grain yields were reduced by 53% and 8%, respectively. AWD maintains superior WUE compared with CF regardless of the type of varieties, suggesting this technique is a drought-adaptive strategy.

Keywords Alternate wetting and drying · Rice variety · Water use efficiency · Dry season rice · Climate model ensembles · Crop model

C. A. Phoeurn (✉) · C. Oeurng · P. Ket
Institute of Technology of Cambodia, Faculty of Hydrology and Water Resources Engineering, Phnom Penh, Cambodia
e-mail: chan.arun@itc.edu.kh

C. Oeurng
e-mail: chanthaposat@yahoo.com

P. Ket
e-mail: pket@itc.edu.kh

C. A. Phoeurn · A. Degré
University of Liège, Gembloux Agro-Bio Tech, Gembloux, Belgium
e-mail: aurore.degre@uliege.be

Introduction

The single food that more people on the planet consume than any other harvest is rice. Nearly 90% of the rice producers and consumers are from Asia. It is grown in over a hundred countries, with a combined harvested area of over 158 million hectares and an annual production of approximately 700 million tons (Sarwar et al., 2022).

Published online: 12 November 2024

Cambodia's economy is narrowly based and driven by four main sectors: garment, tourism, construction, and agriculture. Agriculture, of which rice is the dominant crop, contributes about 24.4% of GDP in 2021 (MAFF, 2022a). Agriculture's gross value added has increased annually by an average of 3 to 4% between 2015 and 2021. Cambodia must increase its rice production twice by 2050 to secure future food security and exportation (MAFF, 2022b). To achieve this goal, there is a need to increase dry-season production, which is currently limited due to water scarcity. Dry-season rice covers only 19% of the paddy land (3.6 million ha) and produced 26.15% of the total paddy yield (wet and dry paddy) of 11,700 million tons between 2023 and 2024 (Sokkea, 2024).

In addition to water scarcity, climate change is another issue for rice producers. The Intergovernmental Panel on Climate Change (IPCC) reports decreased precipitation in the Gulf of Thailand during winter and summer, especially at + 4 °C higher temperatures. These climate risks are expected to lower crop yields and fish harvests, threatening food security in the region, including Cambodia. (FAO 2024). Climate change is projected to reduce total rice production by about 2.5% in 2030 and 9.8% in 2050 (MAFF, 2022b).

Traditional rice cultivation, such as continuous flooding (CF), consumes much water. As a result, cultivated rice fields use about 30% of freshwater resources and 40% of irrigation worldwide (Sarwar et al., 2022). There are plenty of water-saving methods that have been developed to improve water use efficiency (WUE), including raised-bed systems for direct seeding, the system of rice intensification, non-flooded mulching cultivation, aerobic cultivation, and alternate wetting and drying (AWD) irrigation (Carrijo et al., 2017). Fields under AWD are exposed to intermittent drying cycles during the growth season. As soon as the drying criteria are reached, fields are re-ponded (Isafaq et al., 2020). Because of its simplicity of use, AWD is among the most employed water-saving techniques. It has been used and proven to increase WUE worldwide, including in Asia (Arai et al., 2021; Cao et al., 2021; Yao et al., 2012; Sriphirom et al., 2019), Europe (Monaco et al., 2021; Oliver et al., 2019), the USA (Artwill et al., 2023; Runkle et al., 2018), and Africa (de Vries et al., 2010). The above studies claimed 20% to 60% of water saving.

Under potential climate change conditions, rice undergoing the alternate wetting and drying (AWD) cycle may face drought alongside extreme heat. Investigating this hypothesis to confirm the viability of using the AWD method for dry-season rice in Cambodia as an adaptive technique is essential.

Various techniques, including crop modeling, have been employed to investigate the effects of climate change on rice production. Crop simulation models, for example, explore how specific agronomic traits and management practices interact with genotypes and the environment (Raoufi & Soufizadeh, 2020). AquaCrop, a crop water productivity model developed by the Food and Agriculture Organization (Steduto et al., 2012), is among the various models available to assess water-limited crop yields under various environmental and management conditions. The model reasonably accurately predicts crop growth indices and soil, plant, and environment continuum components despite its simplicity. Various studies have demonstrated the capability of the AquaCrop model to simulate the growth of rice under AWD conditions successfully (Xu et al., 2019; Maniruzzaman et al., 2015; Porras-Jorge et al., 2020; Mirfenderski et al., 2021). In Cambodia, AquaCrop was used to predict the yield of lettuce (Ket et al., 2018), maize (Na et al., 2017), and rice (Alvar-Beltrán et al., 2022). Nevertheless, none has attempted to use the model under AWD conditions.

In addition, integrating climate scenarios into crop modeling offers numerous benefits. They allow for measuring climate change's impact on rice production and the probability of specific weather patterns in the areas studied. This information helps prepare for adaptation strategies, such as yield forecasting (Zachow et al., 2023), improving irrigation and fertilizer scheduling (Osman et al., 2022; Shrestha et al., 2014), selecting resilient crop varieties (Osman et al., 2022), selecting planting date (Deb et al., 2015), and mitigating the impact of abiotic stresses on rice yields (Abhishek et al., 2023). In Cambodia, on the other hand, applying a crop model to explore future climate scenarios with adaptation strategies such as the selection of suitable varieties and water management has rarely been explored in dry-season rice (Alvar-Beltrán et al., 2022). Interestingly, global studies investigating climate impacts on rice growth under AWD irrigation are scarce. So far, the only available study by Mirfenderski et al. (2021) is in Iran. Their study

reported that the AWD strategy would be a more effective climate change adaptation than mid-season drainage from crop yield, water productivity (WP), and economic water productivity (EWP) viewpoints. However, their studies did not include a comparison with CF and were limited to old versions of scenarios from the IPCC 5th assessment report. More evidence, especially from other geographic locations, climate conditions, and various cultivars, is required to support AWD irrigation as an adaptive technique for climate change.

Our research fills the literature gap by utilizing the AquaCrop model, together with the latest emission scenarios from the Coupled Model Intercomparison Project Phase 6 (CMIP6), for the first time to test the hypothesis that AWD could be used as a water productivity improvement technique under climate change for the mid-century period (2041–2070) in Cambodia.

Therefore, this paper aims to (1) calibrate and validate AquaCrop on four rice varieties and various irrigation strategies and (2) assess the impact of climate change on yield and WUE of dry-season rice under CF and AWD in Cambodia. In our approach, we conducted a field experiment in Cambodia to parameterize the AquaCrop model. We downscaled data from multi-model ensembles to project future climate and explored how different short-cycle rice varieties and water management would respond to climate change.

Materials and methods

Study area and experiment detail

Crop trials were conducted at the Agricultural Research and Development Institute (CARDI) in Phnom Penh (11°28′ N, 104°48′ E). The region is classified as a tropical climate governed by monsoon winds. Total yearly precipitation varies nationwide, ranging from 1400 to 4000 mm (FAO, 2024). In Cambodia, the average daily maximum temperature (Tmax) is approximately 28 °C, while the average daily minimum temperature (Tmin) is approximately 22 °C. Mean Tmin is consistently above 25 °C during the monsoon season, although mean Tmax may surpass 35 °C during the pre-monsoon months (April and May). The trial was conducted in 2023 during the dry season from January to April.

The experimental site (20×45 m^2) was split into two blocks, with alternate wetting and drying (AWD) and continuously flooded (CF) replicates adjacent to each other. Within each block were individual randomized plots of four rice cultivars and three replications. The size of each plot was 5×5 m^2. The rice varieties included Sen Kra Ob (*SK*), CAR15 (*CAR*), Sen Pidor (*SP*), and check rice: *OM5451* (OM). The varieties were short-cycle, taking between 89 and 100 days after transplanting (DAT) to maturity. A 60:30:30 $N:P_2O_5:K_{2O}$ fertilizer ratio was used.

Plastic film was placed over the bundles to prevent lateral seepage, a crucial factor in the experiment. This film acted as a barrier, ensuring that water did not seep laterally from the main plots. To further control water flow, the blocks were divided by gaps of five meters. During the continuous flooding (CF) regime, the water depth in the entire field was maintained between 1 and 5 cm from 7 days after transplanting until ten days before maturity. In the AWD regime, 35-cm long and 10 cm in diameter hollow PVC tubes were placed vertically in the soil at a depth of 15 cm in each trial. The tube was perforated with holes on all sides. In the AWD cycle, the soil was re-flooded to 5 cm after the field water disappeared from the tube. The cycle began 3 weeks after transplantation and ended 1 week before peak flowering.

Data collection and measurement

Weather data inputs

The daily weather data, such as air temperatures, rainfall, wind speed, relative humidity, and solar radiation, were recorded from an automated weather station (iMETOS 3.3, Pessl Instruments, Werksweg, Weiz, Austria) at the experimental site. Reference evapotranspiration (ETo) was determined using the Penman–Monteith Method.

Irrigation inputs

The pump was connected to tubes that supplied irrigation. The irrigation volume was calculated by multiplying the plot's cross-section area by the water height at the plot's reference point.

Crop inputs

Twenty-one-day-old seedlings were transplanted at 20 cm × 20 cm spacing in each trial. The flowering date was identified as when 50% of the rice plants in a plot started flowering, and the maturity date was calculated as 30 days after flowering. Regular measurements of aboveground biomass and canopy cover were taken over time. Aboveground biomass from 10 plants was harvested biweekly and dried in an oven at 70 °C for 48 h. Canopy cover data was collected weekly through digital photos taken at a consistent height of 1.8 m, with three points per replicate. The fraction of canopy covering the soil was determined by dividing the total number of crop pixels by the total number of picture pixels. To eliminate border effects that can distort images and inflate canopy cover values, three by four plants in the center of the image were retained for analysis. Image analysis was conducted using Adobe Photoshop 2020.

At the point of maturity, 10 randomly selected hills were sampled from a 6 m^2 area to assess grain yield (Y) and total aboveground biomass (B), excluding the first and second row and column of rice plants to mitigate border effects. The harvest index (HI), calculated as the ratio of grain yield to total aboveground biomass, was determined. Grain yield values were adjusted to a standard moisture content of 0.14 g H_2O g^{-1} fresh weight. Once a month, one plant per plot was collected to measure the effective root depth (ERD), defined as the depth at which at least 70% of the roots are concentrated.

Soil inputs

Before planting rice seedlings, soil samples were taken in a column 0.8 m deep from different horizons. Three replicates were collected for each horizon. Hydrometers (ASTM D 422, Eijkelkam, Nijverheidsstraat, EM Giesbeek, Netherlands) were used to identify the soil texture. A pressure plate (1600F1 and 1500 F2, Eijkelkam, Nijverheidsstraat, EM Giesbeek, Netherlands) was used to measure the field capacity and permanent wilting point at pressures of − 33 and − 1500 Kpa, respectively. Soil saturation was derived from the bulk density determined by the ring method. Saturated conductivity was measured by KSAT (Meter Group, Pullman, WA, USA). Teros 12 and Teros 21 (Meter Group, Pullman, WA, USA) were used to measure the hourly volumetric soil moisture content (SMC) and soil tension from the 35th to the 65th day after transplanting (DAT) during the AWD cycle.

Determination of water use efficiency

Water usage efficiency (WUE) is defined as the yield of grain per unit of total water input, which includes irrigation and precipitation.

Description of AquaCrop model

The FAO AquaCrop model simulates crop yield through a series of steps: (i) crop development, (ii) crop transpiration, (iii) biomass production, and (iv) yield formation. Evapotranspiration calculations in the model are split into transpiration, linked to canopy cover (CC), and soil evaporation, which is proportional to bare soil. The CC is multiplied by the reference evapotranspiration (ETo) derived from the Penman–Monteith equation and the crop coefficient (Kc) to determine potential crop transpiration. Actual transpiration (Ta) is then calculated from potential evapotranspiration. Ta is further utilized to compute crop biomass (B) by multiplying it by water productivity (WP) (Eq. 1). The harvest index (HI) is employed to determine crop yield (Y) based on crop biomass (B) (Eq. 2) (Raes et al., 2017):

$$\text{Crop biomass (B)as kg/ha} = \sum \text{Ta} * \text{WP} \quad (1)$$

$$\text{Crop yield(Y)as kg/ha} = \text{HI} * \text{B} \quad (2)$$

Model calibration and validation

The current investigation utilized AquaCrop model version 6.1. Calibration involved using AWD data and comparing it against observed canopy cover (CC), biomass, soil moisture content, and final grain yield for each replicate across all varieties. The model was run individually for each replicate to ensure accuracy. Before calibration, a sensitivity analysis adapted from Geerts et al. (2009) was conducted to identify crucial parameters needing adjustment during calibration. The model's projections were then adjusted through a trial-and-error method, focusing on one input variable at a time, and iteratively repeated until observed

and model-simulated values closely matched for all treatments. Default settings were used for temperature and water stress, with no consideration for fertility or salinity stress.

In the validation phase, calibrated AquaCrop model data was converted to the growing degree days (GDD) mode and tested against CF data. GDD represents the accumulated temperature required for a crop to transition from one phenological stage to another. Using the GDD mode, it is feasible to compare simulated phenology under various future climatic scenarios. The statistical goodness-of-fit indicators used were Percent of deviation (Pd), coefficient of determination (R^2), root mean square error (RMSE), normalized root means square error (nRMSE), and Willmott's index of agreement (d). Percent of deviation (Pd) is determined by the following equation (Eq. 3):

$$Pd = \left(\frac{S_i - M_i}{M_i}\right) \times 100\% \tag{3}$$

where Mi and Si are the observed/measured and simulated values for the irrigation treatment data set.

Lower nRMSE values indicate good agreement between simulated and measured values. Simulation results can be considered excellent if nRMSE is smaller than 10%, good if it is between 10 and 20%, fair if it is between 20 and 30%, and poor if it is larger than 30% (Raes et al., 2012).

Climate data downscaling and bias correction

The dataset known as the NASA Earth Exchange Global Daily Downscaled Projections (NEX-GDDP-CMIP6) consists of climate scenarios that have been downscaled globally from the General Circulation Model (GCM) experiments carried out as part of the Coupled Model Intercomparison Project Phase 6 (CMIP6) (Eyring et al., 2016). These scenarios cover two out of the four primary greenhouse gas emissions pathways referred to as Shared Socioeconomic Pathways (SSPs) (Meinshausen et al., 2020; O'Neill et al., 2016). The CMIP6 GCM runs were created for the Sixth Assessment Report of the Intergovernmental Panel on Climate Change (IPCC AR6). This dataset contains downscaled projections from ScenarioMIP models distributed through the Earth System Grid Federation (O'Neill et al., 2016).

NEX-GDDP-CMIP6 was used to obtain possible projections of future climate variables for the period 2041–2070. We adopted two shared socioeconomic pathways (SSP3-7.0 and SSP5-8.5) to represent medium and high greenhouse gas emissions. For each scenario, we applied four different GCMs, including EC-Earth3, FGOALS-g3, MIROC6, and MPI-ESM1-2-LR. The ETo for baseline and future data was estimated from T maximum and T minimum using the FAO-Penman–Monteith equation as described in Allen et al. (1998).

Though the NEX-GDDP-CMIP6 dataset was globally bias-corrected (Maurer et al., 2008; Thrasher et al., 2012), the application of correction using data from the actual site would significantly improve the errors. The linear scaling approach has proved its capability for bias correction of climate data (Daniel, 2023; Shrestha et al., 2017) and was adopted in this study. The CIMP6 dataset was adjusted for bias, utilizing baseline data T maximum, T minimum, and precipitation data from historical records spanning 1996 to 2011. The baseline data was from the nearby station (Pochentong Station: 104°50′, 11°33′, altitude 11 m) obtained from the Ministry of Water Resources and Meteorology (MOWRAM). In the linear scaling approach outlined in Eq. (5), the future CIMP6 data, such as precipitation is corrected with a multiplier, and the temperature is adjusted by the additive term:

$$P^{C}_{f,m,d} = P_{f,m,d} \times \frac{\mu(P_{ob,m})}{\mu(P_{h,m})} \tag{4}$$

$$T^{C}_{f,m,d} = T_{f,m,d} \times \left[\mu(T_{ob,m}) - \mu(T_{h,m})\right] \tag{5}$$

where $P_{f,m,d}$ and $T_{f,m,d}$ denote the future precipitation and temperature, respectively; $P_{h,m,d}$ and $T_{h,m,d}$, respectively, denote the historical precipitation and temperature from the original RCM outputs; $P_{ob,m}$ and $T_{ob,m}$ denote the observed historical precipitation and temperature; the subscripts d and m are specific days and months, respectively; C denotes the corrected value; and μ denotes the mean value.

Statistical analysis

R (version 4.2.2) was used to analyze the future data, and an analysis of variance (ANOVA) was done at a 95% significance level.

Result and discussion

Result

Model parameterization

Table 1 displays the calibrated parameters and their respective sensitivity levels. From the sensitive analysis, the initial soil condition, WP, and HI had a notable impact on Y and B, while Ksat was identified as a critical factor affecting SMC. Furthermore, stress factors such as canopy expansion, early senescence, and stomatal closure were low sensitive since the soil moisture and tension levels in this study had never experienced a drop below field capacity, as shown in Fig. 1. Therefore, these parameters were set to default.

Most of the model inputs were derived from averaging direct measurements, as detailed in Sect. "Data collection and measurement". The values for plant density, time to achieve maximum canopy cover, flowering duration, maximum ERD, and time taken to reach maximum ERD were consistent across all varieties. However, differences were noted in the observed values for HI, recovery time, maximum canopy cover (CCx), initial canopy cover (CCo), canopy size seedling, time to flowering, and maturity across the various varieties.

The different varieties exhibited varying values for WP, CCo, seedling canopy size, and time to recovery. While canopy decline typically occurred in less than a week, it was set at 9 days, which is the minimum value allowed by AquaCrop. The rate of decline influenced the time to senescence. Effective root depth (ERD) ranged from 4 to 13 cm, but AquaCrop allowed a minimum depth of 10 cm. In cases where ERD fell below 10 cm, it was fixed at 10 cm for the entire season. The maximum canopy cover (CCx) ranged from 50 to 65% for all varieties and was usually achieved around 45 days after transplanting (DAT) during the flowering stage. These values were then used for model parameterization.

Model calibration and validation

Grain yield and final biomass

The results in Table 2 confirm the model's accuracy in simulating grain yield (Y) and biomass (B) within an acceptable range. The grain yield (Y) measured for different rice varieties ranged from 2.28 to 5.1 tons/ha under both irrigation management. The model's estimated grain yield for the genotypes fell within the 2.61 to 5.12 tons/ha range. Notably, OM displayed the highest yield, while SK exhibited the lowest. The measured biomass (B) for various rice varieties ranged from 7.91 to 11.03 tons/ha under both irrigation management, while the modeled values ranged from 9.34 to 11.47 tons/ha. CAR, OM, and SP varieties had comparable B, with SK presenting the lowest B.

During calibration and validation, the prediction errors for Y ranged from − 4.36 to 11.49% and 1.59 to 24.38%. In contrast, B production ranged from − 0.39 to 5.67% and − 3.23 to 18.98%. However, the SP variety notably showed the highest relative error in model validation for B and Y.

Despite these variations, the model's overall accuracy in simulating grain yield and biomass production is evident.

CC and time series B

The model was calibrated using field data collected in the AWD regime. Generally, the calibrated CC and time series B matched the measured values well (see Fig. 2). The average goodness-of-fit metrics obtained for modeling CC and time series B for the four varieties were as follows: $R2 > 0.93$, $D > 0.94$, and $RMSE < 15\%$ for CC and $R2 > 0.95$, $D > 0.94$, and $RMSE < 1.5$ tons/ha for B. The nRMSE of calibrated CC indicated a good fit (nRMSE = 17.5–27%). This suggests that the model calibration is robust. While the model accurately simulated CC patterns, it underestimated B by 25–33.5%. This predictive error in simulating B for all rice varieties during the grain-filling stage was attributed to the substantial increase in total B weight.

The figures in Fig. 3 depict indicators showing how closely the validated model matches the actual field observations. The average goodness-of-fit metrics for validating CC and time series B of the four varieties were as follows: $R2 > 0.95$, $D > 0.92$, and $RMSE < 15\%$ and $R2 > 0.98$, $D > 0.92$, with $1 < RMSE < 2.2$ tons/ha. The nRMSE for the validated CC of the three varieties indicated a good fit ($nRMSE < 20\%$), except for OM, where the nRMSE was 32.5%. This discrepancy occurred because the

Table 1 Parameters used for calibrating AquaCrop model

Inputs	Units	Value observed (calibrated)				Sensitivity
		CAR	*OM*	*SK*	*SP*	
1. Crop						
Plant density	Plants/ha	250,000	250,000	250,000	250,000	
Type of planting method	-	Transplanting	Transplanting	Transplanting	Transplanting	
Initial canopy cover (CC_o)	%	(1.50)	(1.00)	(1.13)	(1.50)	Low
Canopy size seedling	cm2/plant	(5)	(4)	(4.5)	(6)	Moderate
Canopy decline	Days	(9)	(9)	(9)	(9)	Moderate
Time to recovery	Days	(7)	(10)	(7)	(10)	Low
Time to maximum canopy cover	Days	45	45	45	45	Moderate
Time to senescence	Days	(85)	(80)	(90)	(86)	-
Time to maturity	Days	94	89	99	93	-
Maximum canopy cover (CCx)	%	75	65	58	66	Moderate
Time to flowering	Days	64	59	69	63	Low
Duration of the flowering	Days	7	7	7	7	-
Max. effective rooting depth	cm	11–13 (10)	11–13 (10)	11–13 (10)	11–13 (10)	Low
Time for maximum root depth	Days	94 (CST)	45 (CST)	45 (CST)	70 (CST)	Low
Crop water productivity (WP*)	kg/m^3	(16)	(19)	(15)	(16)	High
Harvest index (HI)	%	38	50	28	41	High
water stress: Default value						
Effect of crop transpiration (KcTr)	-	1.1	1.1	1.1	1.1	-
Canopy expansion	-	Extremely sensitive to water stress	Extremely sensitive to water stress	Extremely sensitive to water stress	Extremely sensitive to water stress	Low
Stomatal closure	-	Moderately sensitive to water stress	Moderately sensitive to water stress	Moderately sensitive to water stress	Moderately sensitive to water stress	Low
Early canopy senescence	-	Moderately sensitive to water stress	Moderately sensitive to water stress	Moderately sensitive to water stress	Moderately sensitive to water stress	Low
Heat stress: default value						
Base temperature		8	8	8	8	-
Upper temperature		30	30	30	30	-
Start of heat-stress effect		35	35	35	35	-
Maximum heat-stress effect		40	40	40	40	-
2. Field						
Surface practice		Soil bund 0.25 m	Soil bund 0.25 m	Soil bund 0.25 m	Soil bund 0.25 m	-

Table 1 (continued)

Inputs	Units	Value observed (calibrated)				Sensitivity
		CAR	*OM*	*SK*	*SP*	
3. Soil profile						
Layer 1: 0—0. 3 m						
Texture		Sandy loam	Sandy loam	Sandy loam	Sandy loam	-
PWP (V%)		9.6 ± 2.8	9.6 ± 2.8	9.6 ± 2.8	9.6 ± 2.8	Moderate
FC (V%)		29 ± 2 (39)	29 ± 2 (39)	29 ± 2 (39)	29 ± 2 (39)	Moderate
SAT (V%)		39 ± 1 (45)	39 ± 1 (45)	39 ± 1 (45)	39 ± 1 (45)	Moderate
Ksat (mm/d)		169 ± 97 (4)	169 ± 97 (4)	169 ± 97 (4)	169 ± 97 (4)	Hight
Layer 2: 0.3–0. 4 m						
Texture		Sandy loam	Sandy loam	Sandy loam	Sandy loam	-
PWP (V%)		10 ± 2.8	10 ± 2.8	10 ± 2.8	10 ± 2.8	Moderate
FC (V%)		23 ± 1 (32)	23 ± 1 (32)	23 ± 1 (32)	23 ± 1 (32)	Moderate
SAT (V%)		36 ± 4 (38)	36 ± 4 (38)	36 ± 4 (38)	36 ± 4 (38)	Moderate
Ksat (mm/d)		5.5 ± 1.2 (7)	5.5 ± 1.2 (7)	5.5 ± 1.2 (7)	5.5 ± 1.2 (7)	Hight
Layer 3: 0.4–0. 8 m						
Texture		Sandy loam	Sandy loam	Sandy loam	Sandy loam	-
PWP (V%)		9.5 ± 1.5	9.5 ± 1.5	9.5 ± 1.5	9.5 ± 1.5	Moderate
FC (V%)		22 ± 3	22 ± 3	22 ± 3	22 ± 3	Moderate
SAT (V%)		37 ± 4	37 ± 4	37 ± 4	37 ± 4	Moderate
Ksat (mm/d)		2.4 ± 1.9 (3)	2.4 ± 1.9 (3)	2.4 ± 1.9 (3)	2.4 ± 1.9 (3)	Hight
4. Initial condition						
Soil moisture content		Saturated	Saturated	Saturated	Saturated	Hight

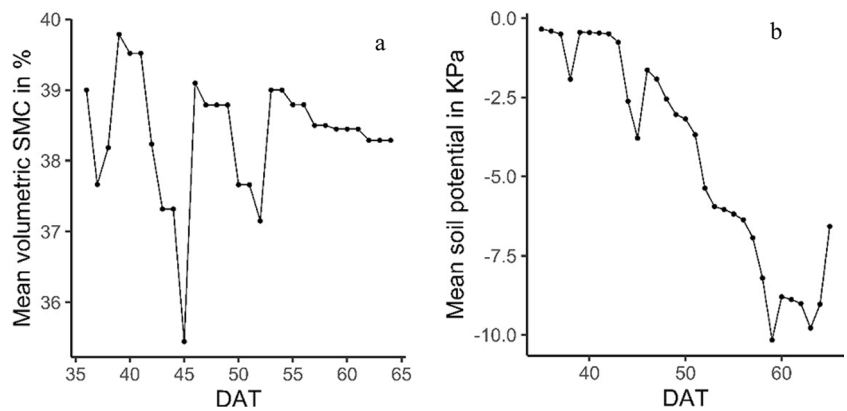

Fig. 1 (**a** Mean observed VSMC and **b** mean observed soil potential during AWD cycle

measured CC values in CF conditions were lower than in AWD conditions throughout the season. However, the poor fitting of OM did not impact the accuracy of the model's simulation for grain yield and final biomass.

Similarly, during the validation phase, like in the calibration phase, AquaCrop accurately simulated CC patterns but underestimated B by 22–45.2%. This underestimation was mainly due to the substantial increase in rice biomass during the grain-filling stage.

Table 2 Calibration and validation results of simulating biomass and grain yield production of the four varieties. Standard deviations are given in brackets

	Grain yield (tons/ha)			Biomass (tons/ha)		
	Obs	**Sim**	**Pe (± %)**	**Obs**	**Sim**	**Pe (± %)**
Calibration						
AWD						
CAR	4.12 (0.46)	4.06	10.30 (5.36)	10.67 (0.68)	10.85	5.67 (4.23)
OM	5.1 (0.27)	4.86	−4.36 (5.33)	10.7 (0.2)	10.13	−5.32 (1.79)
SP	4.44 (0.24)	4.23	−4.51 (5.31)	10.32 (0.58)	10.28	−0.39 (0.5)
SK	2.28(0.27)	2.5	11.49 (14.26)	8.55 (0.25)	9.5	5.31 (3.05)
Validation						
CF						
CAR	3.86 (0.33)	4.29*	8.88 (8.94)	10.33 (0.87)	11.47	8.68 (8.89)
OM	5.04 (0.18)	5.12	1.59 (4.02)	11.03 (0.58)	10.67	−3.23(4.94)
SP	3.63 (0.31)	4.48	24.38 (10)	9.19 (0.19)	10.93	18.98 (2.39)
SK	2.4 (0.21)	2.61	12.23 (11.46)	7.91 (1.2)	9.34	18.01 (1)

*The simulating biomass and grain yield remained the same for each replication

Despite these challenges, the indices for CC and B in the validation phase indicated an acceptable model prediction.

Soil moisture content

Though the model mimicked the soil moisture better in the calibration than validation (Fig. 4), R^2 and D values were in the acceptable range of $R^2 > 0.5$, $D > 0.5$, and nRMSE < 10%. In calibration, we achieved $R^2 = 0.51$, RMSE = 4.25%, nRME = 5.55%, and D = 0.51. In validation, we achieved $R^2 = 0.54$, RMSE = 4.73%, nRME = 6.2%, and D = 0.57.

Overview of future climate

Variability in mean monthly minimum and maximum temperature, ETo, and rainfall in the future (2041–2070) at CARDI under two climatic scenarios is shown in Fig. 5. The temperature indicated a lowering trend from May to January and an increasing trend from February to April, according to the overall baseline trends and future estimates for Tmax and Tmin (Fig. 5a and 5b). In comparison to the baseline (1996–2011), the monthly temperature would rise on average by 0.88 °C (Tmin) and 1.33 °C (Tmax) under the SSP3-7.0 scenarios and by 0.99 °C (Tmin) and 1.36 °C (Tmax) under the SSP5-8.5 scenario. April showed the baseline highest minimum of 25.58 °C and maximum temperature of 35.54 °C, which were slightly close to the heat stress zone. The mean Tmax and Tmin of April were projected to increase by 0.96 and 1.23 °C for SSP3-7.0 scenarios and by 0.76 and 1.27 °C for SSP5-8.5 scenarios, respectively. Typically, the driest months occur during the dry-season rice growing period, which falls between March and May. During this time, the monthly baseline ETo ranged from 135 to 160 mm (Fig. 5c). While the mean ETo values for both the baseline and future periods were not much different, there was an expected increase in ETo in the future, with maximum values projected to reach up to 195 mm (a 31% increase) per month in April. Figure 5d illustrates a rising trend in rainfall across all months, with average values of 5.62 mm (4%) and 11.25 mm (9%) for SSP3-7.0 and SSP5-8.5, respectively. However, the future monthly rainfall from December to April would be lower than the total monthly ETo, indicating the need for additional water input to ensure the health of the rice plants.

Future impact of climate change on rice growing and WUE

The simulations of the effect of future climatic conditions on maturity, grain yield, crop damage, biomass, HI, and WUE under two water regimes for the mid-century (2041–2070) are shown in Fig. 6. Figure 6a illustrates the effect of future climatic conditions on the maturity of the four rice cultivars. The projected maturity dates for varieties *OM, CAR*, and *SP* were expected to be earlier by 0.8–2.4 days (CF) and 1.2–5.19 days (AWD) under SSP3-7.0, while delays of 0.36 to 2.66 days were anticipated for both regimes

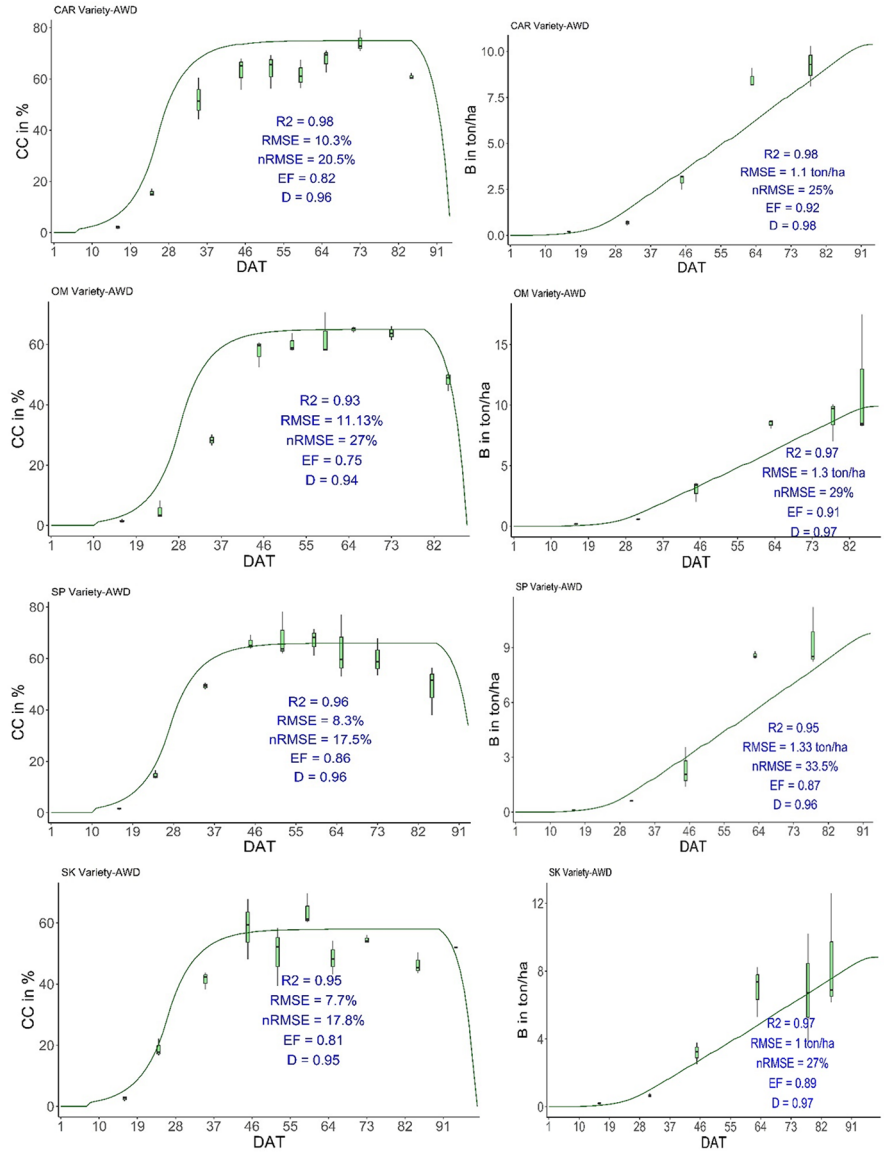

Fig. 2 Simulated and measured canopy cover (CC) and time series B for the calibration under AWD regime. Error bars indicate the standard deviation across replicated measurements

under SSP5-8.5. In contrast, the days to maturity for variety SK were projected to be delayed by 5.17 days (SSP3-7.0) and 6–7.82 days (SSP5-8.5) under both regimes.

Compared with the baseline, the simulated average grain yield of *SK* showed a substantial reduction of approximately 53%, followed by *CAR*, which showed around an 8% decrease under future climate change scenarios across both water management approaches. Conversely, under both scenarios, *OM* and *SP* in both regimes demonstrated an increase in average grain yield of 18% and 14%, respectively (Fig. 6b).

According to Fig. 6c, the likelihood of crop damage incidents under both regimes was estimated at 17% (SSP3-7.0) and 9% (SSP5-8.5) for *CAR* and 23.5% (SSP3-7.0) and 17% (SSP5-8.5) for SK. The crop damage for SP and OM was not anticipated under SSP3-7.0. Under SSP5-8.5, the damage of 1.2% for SP and 0.8% for OM was expected.

In Fig. 6d, it was observed that the simulated average WUE of *SK* experienced a significant reduction of about 54%, followed by *CAR* with an approximately 8.3% decrease under future climate change scenarios across both water management strategies.

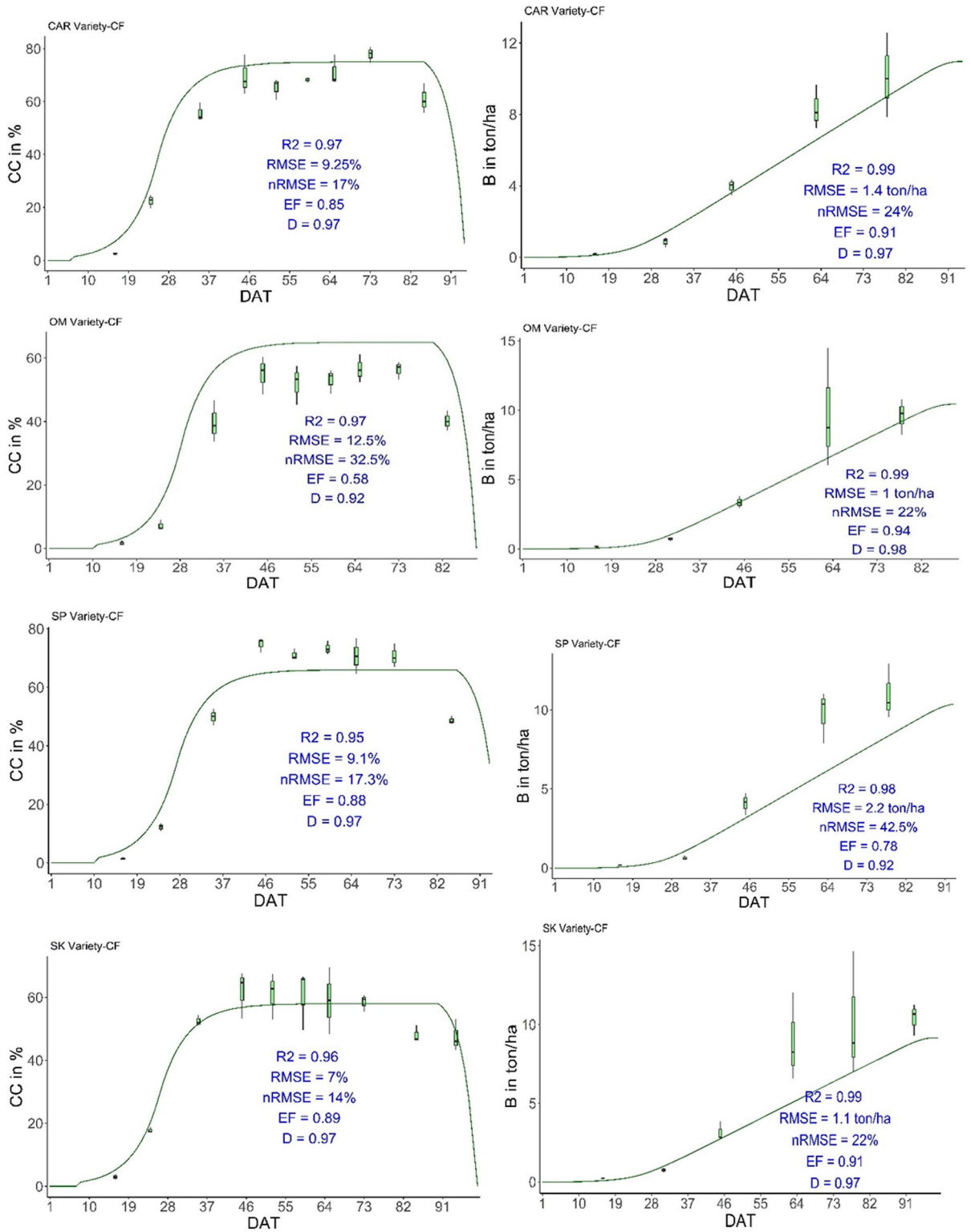

Fig. 3 Simulated and measured canopy cover (CC) and time series B for the validation under CF regime. Error bars indicate the standard deviation across replicated measurements

In contrast, under both scenarios, *OM* and *SP* in both regimes exhibited an increase in average WUE of around 19% each. However, under any condition, the simulated average WUE of AWD15 surpassed that of CF under both future scenarios across all varieties and regimes. Under SSP3-7.0, the WUE of AWD was between 22 and 26% higher than those grown under CF, while under SSP5-8.5, the WUEs of AWD were between 18 and 25% greater. Except for *SK* (Fig. 6e), all varieties were projected to experience an increase in average biomass ranging from 16 to 22% under future climate change scenarios across both water management approaches. However, the reduction in SK's biomass was minimal, approximately 1.5 tons. ha^{-1} across all scenarios and regimes. As a result of the increased biomass, a decrease in average HI was simulated under future climate change scenarios across all varieties and regimes (Fig. 6f). Regardless of water regime and climate scenarios, the simulated average HI was reduced by 54.2%, 23%, 3.5%, and 1.5% for *SK*, *CAR*, *SP*, and *OM*, respectively.

Discussion

AquaCrop performance for growth simulation in AWD and CF

Grain yield (Y) and total aboveground biomass (B)

Given the significant influence of variety, it is essential to calibrate the model against specific varieties for accurate simulation (Steduto et al., 2012). AquaCrop successfully simulated rice varieties' yield (Y) and biomass (B) using different water management strategies. The percent of deviation (Pd) between the simulated and observed Y and B values was outstanding, consistent with other studies using AquaCrop for rice growth under AWD and water stress conditions (Maniruzzaman et al., 2015; Mirfenderski et al., 2021; Vahdati et al., 2020). However, the model overestimated Y and B of SP variety in the validated model (CF regime) due to differences in the measured values between both treatments.

CC and time series B and CC

The simulation results showed that AquaCrop effectively captured the development of crop canopies across all treatments and varieties. It was demonstrated through a variety of statistical measures that were calculated. In general, the metrics of time series CC indicated good performance by the calibrated and validated model, as cited in AquaCrop studies by Maniruzzaman et al. (2015) and Raoufi et al. (2018). However, AquaCrop did not capture the CC growth for OM well, which is the improved variety. The nRMSE of OM was the highest compared to the three local varieties. This difference could be due to local growth behavior and improved variety (Saito et al., 2006). This finding contrasted with the finding of Raoufi et al. (2018), who observed a poorer prediction of CC in the local variety than the improved one. This model may require further investigation to differentiate between the canopy development of local and improved cultivars.

In general, the metrics of time series B indicated good to fair performance by the calibrated model, as cited in AquaCrop studies by Maniruzzaman et al. (2015) and Raoufi et al. (2018). Nonetheless, the normalized root mean square error (nRMSE) was higher than in those studies due to the substantial increase in total B weight during the grain-filling stage, primarily driven by the weight of the grains. The bias between observation and simulation in the grain-filling stage varied between 30 and 40%. We tried to reduce such a bias by increasing the CCo and Canopy size seedling, which caused a slight overestimation of time series CC at the early growing stage. In addition, increasing B to fit the measured value also led to a considerable bias in the final Y and B. Thus, we restricted the fitting in the way that the final Y and B were most fitted to the observed values, as these two variables were critical factors for the future climate projection.

This means the model's ability to simulate B for the selected type of varieties during the grain-filling stage needs improvement. The model's inability to distinguish grain yield density from total biomass at this stage limits its accuracy. However, an option is available and recommended by AquaCrop to update unexpected growth or damage (Raes et al., 2017). This adjustment is inconvenient during the numerous future climate projections under multiple scenarios. Therefore, model improvements that incorporate development rates of grain yield after the flowering stage would be highly desirable to enable the application of the calibrated model across a broader range of genetic conditions. This model weakness was not

problematic for CC because CC became stable from 45 DAT and started reducing during the grain falling stage. Furthermore, the increase in time series B after flowering was due to the increasing weight of grain rather than the rice canopy, which had nothing to do with CC.

However, the imperfection of time series CC and time series B did not influence the final Y and B since we can calibrate WP to compromise the errors. The calibrated WP values were between 15.0 and 19.0 g m^{-2}, which falls within the range (15–20 g m^{-2}) recommended for C3 crops by Raes et al. (2009).

Soil moisture content

The calibration and validation of SMC were only fair (R and D > 0.5; NRMSE < 10%). Since our paddy sub-soil was mostly near saturation, this agreed with the finding of Xu et al. (2019), whose AWD method was irrigating the field to saturation but not flooding. However, Perros-Jorge et al. (2020) better predicted when the soil was drier (soil potential between − 10 and − 20 kPa). In addition, while our experiments did not present severe water stress conditions on the crop, we did not see any gradient in model performance with the degree of water stress.

Impact of climate change on short-cycle rice during mid-century

In comparison to the baseline (1996 − 2011), projected temperature increases were expected to increase on average 0.93 °C for Tmin and 1.35 °C for Tmax under both SSP3-7.0 and SSP5-8.5 scenarios, with notable spikes in March and April, where temperatures could exceed 40 °C. As per Raes Dirk (2017), heat stress in rice is triggered between 35 and 40 °C. Fahad et al. (2016) suggested a 10% decline in rice grain yield for each 1 °C rise in growing-season minimum temperature during the dry season. While rainfall was forecasted to rise by 4–9% monthly, ETo demand in April also would increase by 31%, posing a severe threat to crops if cultivated during that period. This month coincides with our experiment period, which ran from late January to April.

Each short-cycle rice variety displayed distinct flowering times and growth durations in our experiment. The impact of climate change was most pronounced on the yield, HI, and WUE of the *CAR* and *SK* varieties, which had more extended growth periods than the other two varieties. The impact of water shortage during the projection was less critical, as rice growth under full irrigation also suffered the same damage. *SK*, having the most extended growing period (99 days) in particular, faced significant exposure to heat stress conditions (Tmax ≥ 35 °C) among the short-cycle varieties. While *CAR* had a mean maturity of one day longer time to flower than SP, it experienced severe damage, which may be due to high temperature. This finding aligns with previous research findings indicating that prolonged exposure to high temperatures greater than 35 °C during flowering, even from 1 h to a day, can lead to spikelet sterility (Devkota et al., 2013; Shi et al., 2016; Van Oort & Dingkuhn, 2021). Short-cycle varieties with growing periods of less than 93 days, such as *OM* and SP in our case, were not affected by heat stress. However, under the highest emission scenario, SSP5-8.5, the overall risk of damage for these two varieties was very low, about 3–6%, regardless of water management.

Due to its correlation with yield, WUE was observed to increase in *the SP and OM varieties* but decrease in *CAR* and *SK*. AWD maintained superior WUE compared to CF throughout. This highlights AWD's potential as a drought-adaptive strategy going forward, maintaining yields while reducing water input for short-cycle rice varieties under 93 days. Interestingly, biomass showed low sensitivity to heat in our study, indicating that climate change impacts grain yield more than biomass.

Conclusions

AquaCrop demonstrated considerable potential in simulated rice varieties and water management. Under medium and high emission scenarios, the frequency of heat stress on rice would happen quite frequently in Cambodia when the maximum temperature exceeds the rice's tolerance level below 35 °C. The ensemble projection indicated that rice grown longer than 93 DAT is more prone to damage. In our case, *Sen Kra* Ob experienced a significant reduction of about 54%, followed by *CAR15* with an approximately

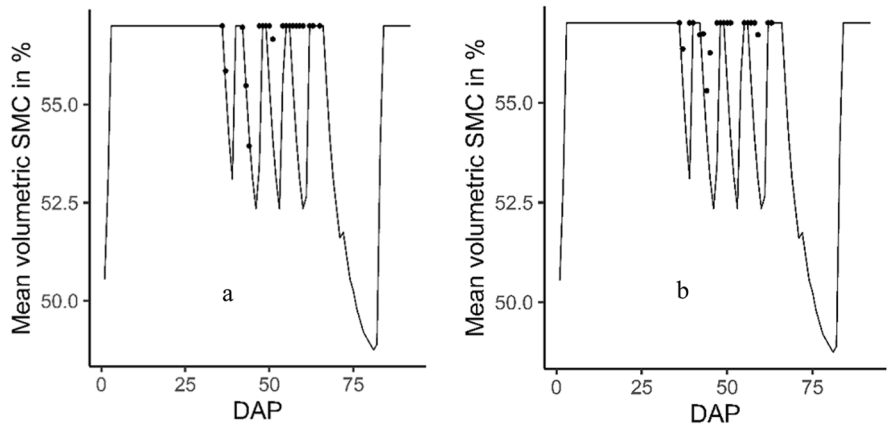

Fig. 4 Simulating and observed SMC for the calibration (four plots) and validation (four plots) under AWD regime

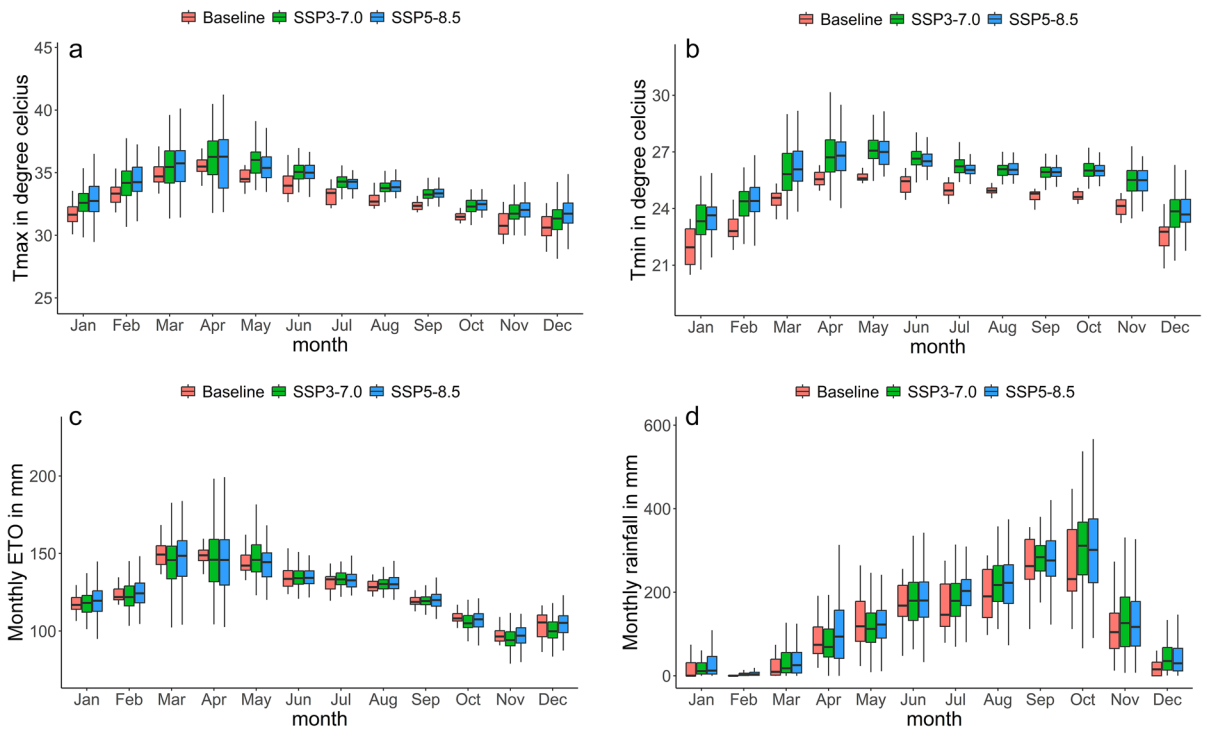

Fig. 5 Projected changes in surface air temperature (**a,b**), ETo (**c**), and rainfall (**d**) under SSP3-7.0 (Medium emission trajectory) and SSP5-8.5 (highest emission trajectory) scenarios for 2041–2070 for the baseline period 1996–2011. Solid lines indicate medians

8.3% decrease under future climate change scenarios across both water management strategies.

OM5451 and *Sen Kra Ob* are the suitable varieties to adapt to climate change. Regarding WUE, AWD is a promising technique for saving water in the future.

To effectively address the challenges posed by climate change in rice production, it is crucial to prioritize the selection of rice varieties with traits that enhance climate resilience and support efficient water management. It is essential to acknowledge that this study was conducted at a field experimental level, and further research is necessary to validate these findings across a broader range of rice varieties and on a larger scale. Additionally, a more thorough investigation into the water stress coefficient for rice varieties under more severe AWD conditions is recommended,

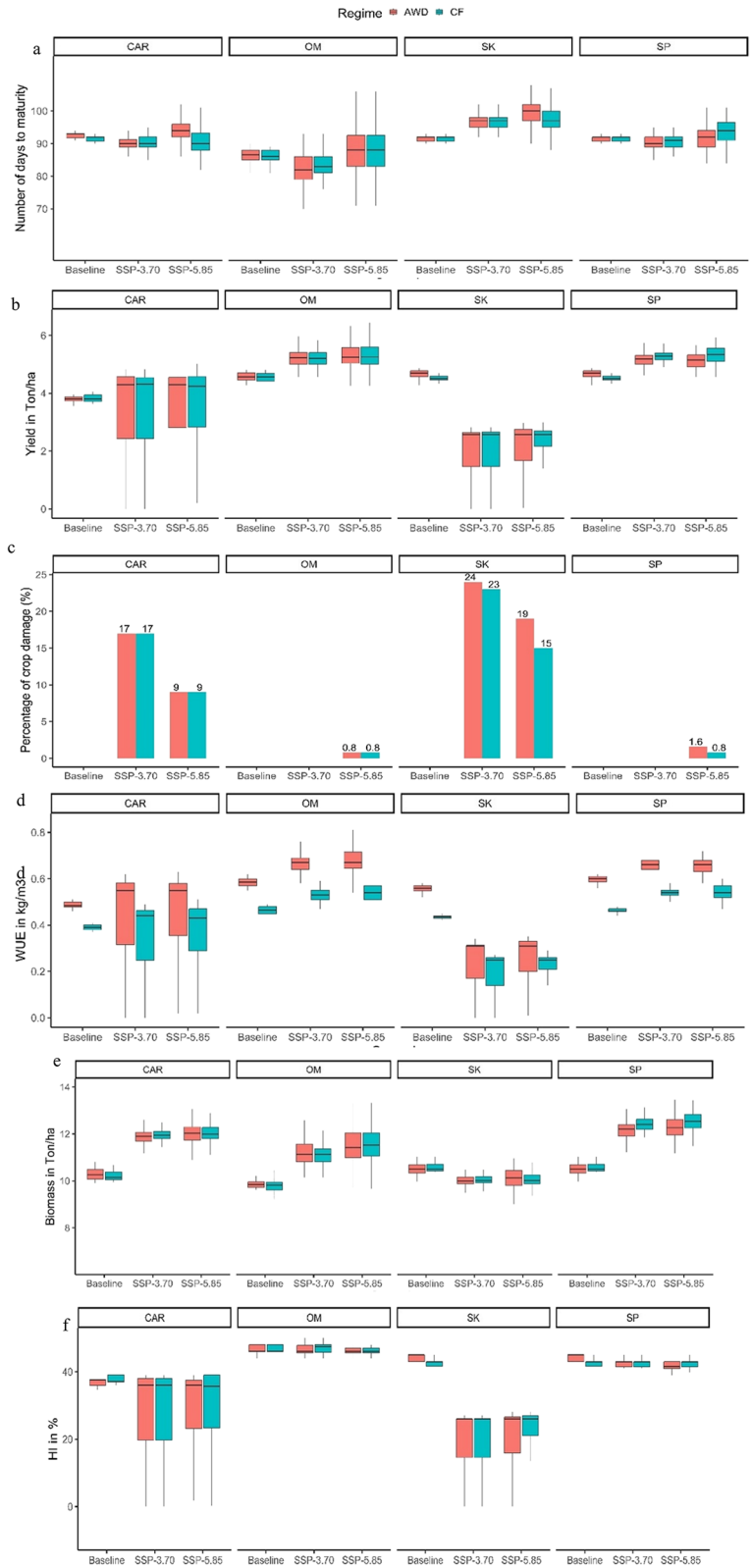

Fig. 6 Simulated days to maturity (**a**), grain yield (**b**), percentage of damage (**c**), WUE (**e**), biomass (**e**), and HI (**f**) of the four rice varieties in historical weather data and two climate change scenarios (SSP3-7.0 and SSP5-8.5) in 2041–2070. Solid lines indicate medians. The percentage of crop damage equals the number of damaged years divided by 120 (30 years * 4 GCM)

as this aspect could not be explored in the current study. Nevertheless, the results suggest that AWD shows promising potential as a climate adaptation strategy for dry-season rice cultivation in Cambodia.

Acknowledgements We are particularly grateful to Dr. Sok Ty and Dr. Chhin Rathana for their assistance with the bias correction analysis and downscaling technique, PEAR LAB and Soil LAB of ITC to provide space and consumables, and CARDI personnel who supported our experiment. This work is part of the PhD of Chan Arun Phoeurn, under a double degree program between the Institute of Technology of Cambodia and the University of Liege, Belgium.

Author contribution Chan Arun Pheourn: conducted the whole experiment, collected data, analyzed the data, and wrote the manuscript. Dr.Aurore Degre and Dr. Pinnara Ket: Provide input for the manuscript, guidance, and review. Dr. Chantha Oeung: provided initial inputs during the experimental design phase.

Funding This study was funded by the Cambodia Higher Education Improvement Project (Credit No. 6221-KH) under Ministry of Education, Youth, and Sport.

Data availability The Excel sheet that summarizes the climate-model ensembles can be found at this link: https://docs.google.com/spreadsheets/d/1wJA7Kd8-rBBH2malQ7RXhNcR62ak2TAz/edit?usp=sharing&ouid=111,915,375,082,130,324,628&rtpof=true&sd=true.

Declarations

Competing interests The authors declare no competing interests.

References

Abhishek, A., Phanikumar, M. S., Sendrowski, A., Andreadis, K. M., Hashemi, M. G., Jayasinghe, S., Prasad, P. V., Brent, R. J., & Das, N. N. (2023). Dryspells and minimum air temperatures influence rice yields and their forecast uncertainties in rainfed systems. *Agricultural and Forest Meteorology, 341*, 109683. https://doi.org/10.1016/j.agrformet.2023.109683

Allen, RG., Pereira, LS., Raes, D., Smith, M. (1998). Crop evapotranspiration. In Guidelines for computing crop water requirements. Irrigation and drainage (pp. 56). FAO.

Alvar-Beltrán, J., Soldan, R., Ly, P., Seng, V., Srun, K., Manzanas, R., Franceschini, G., & Heureux, A. (2022). Modelling climate change impacts on wet and dry season rice in Cambodia. In Journal of Agronomy and Crop Science (Vol. 208, Issue 5, pp. 746–761). Wiley. https://doi.org/10.1111/jac.12617

Arai, H., Hosen, Y., Chiem, N. H., & Inubushi, K. (2021). Alternate wetting and drying enhanced the yield of a triple-cropping rice paddy of the Mekong Delta. In Soil Science and Plant Nutrition (Vol. 67, Issue 4, pp. 493–506). Informa UK Limited. https://doi.org/10.1080/00380768.2021.1929463

Atwill, R. L., Spencer, G. D., Bond, J. A., Walker, T. W., Phillips, J. M., Mills, B. E., & Krutz, L. J. (2023). Establishment of thresholds for alternate wetting and drying irrigation management in rice. In Agronomy Journal (Vol. 115, Issue 4, pp. 1735–1745). Wiley. https://doi.org/10.1002/agj2.21366

Cao, X. C., Wu, L. L., Lu, R. H., Zhu, L. F., Zhang, J. H., & Jin, Q. Y. (2021). Irrigation and fertilization management to optimize rice yield, water productivity and nitrogen recovery efficiency. *Irrigation Science, 39*(2), 235–249. https://doi.org/10.1007/s00271-020-00700-4

Carrijo, D. R., Lundy, M. E., & Linquist, B. A. (2017). Rice yields and water use under alternate wetting and drying irrigation: A meta-analysis. In Field Crops Research (Vol. 203, Issue March). Elsevier B.V. https://doi.org/10.1016/j.fcr.2016.12.002

Daniel, H. (2023). Performance assessment of bias correction methods using observed and regional climate model data in different watersheds, Ethiopia. In Journal of Water and Climate Change (Vol. 14, Issue 6, pp. 2007–2028). IWA Publishing. https://doi.org/10.2166/wcc.2023.115

de Vries, M. E., Rodenburg, J., Bado, B. V., Sow, A., Leffelaar, P. A., & Giller, K. E. (2010). Rice production with less irrigation water is possible in a Sahelian environment. In Field Crops Research (Vol. 116, Issues 1–2, pp. 154–164). Elsevier BV.

Deb, P., Tran, D. A., & Udmale, P. D. (2015). Assessment of the impacts of climate change and brackish irrigation water on rice productivity and evaluation of adaptation measures in Ca Mau province, Vietnam. In Theoretical and Applied Climatology (Vol. 125, Issues 3–4, pp. 641–656). Springer Science and Business Media LLC. https://doi.org/10.1007/s00704-015-1525-8

Devkota, K. P., Manschadi, A. M., Devkota, M., Lamers, J. P. A., Ruzibaev, E., Egamberdiev, O., Amiri, E., & Vlek, P. L. G. (2013). Simulating the impact of climate change on rice phenology and grain yield in irrigated drylands of Central Asia. In Journal of Applied Meteorology and Climatology (Vol. 52, Issue 9, pp. 2033–2050). American Meteorological Society. https://doi.org/10.1175/jamc-d-12-0182.1

Eyring, V., Bony, S., Meehl, G. A., Senior, C. A., Stevens, B., Stouffer, R. J., & Taylor, K. E. (2016). Overview of the Coupled Model Intercomparison Project Phase 6 (CMIP6) experimental design and organization. In Geoscientific Model Development (Vol. 9, Issue 5, pp. 1937–1958). Copernicus GmbH. 10.5194/gmd-9-1937-2016

Fahad, S., Hussain, S., Saud, S., Hassan, S., Ihsan, Z., Shah, A. N., Wu, C., Yousaf, M., Nasim, W., Alharby, H., Alghabari, F., & Huang, J. (2016). Exogenously applied plant growth regulators enhance the morpho-physiological growth and yield of rice under high temperature. In Frontiers in Plant Science (Vol. 7). Frontiers Media SA. https://doi.org/10.3389/fpls.2016.01250

Food and Agriculture Organization (FAO). (2024). Country brief. Office of Climate Change, Biodiversity, and Environment.

Geerts, S., Raes, D., Garcia, M., Miranda, R., Cusicanqui, J. A., Taboada, C., Mendoza, J., Huanca, R., Mamani, A., Condori, O., Mamani, J., Morales, B., Osco, V., & Steduto, P. (2009). Simulating yield response of Quinoa to water availability with AquaCrop. In Agronomy Journal (Vol. 101, Issue 3, pp. 499–508). Wiley. https://doi.org/10.2134/agronj2008.0137s

Ishfaq, M., Farooq, M., Zulfiqar, U., Hussain, S., Akbar, N., Nawaz, A., & Anjum, S. A. (2020). Alternate wetting and drying: A water-saving and ecofriendly rice production system. In Agricultural Water Management (Vol. 241, p. 106363). Elsevier BV. https://doi.org/10.1016/j.agwat.2020.106363

Ket, P., Garré, S., Oeurng, C., Hok, L., & Degré, A. (2018). Simulation of crop growth and water-saving irrigation scenarios for lettuce: A monsoon-climate case study in Kampong Chhnang. *Cambodia. Water, 10*(5), 666. https://doi.org/10.3390/w10050666

Maniruzzaman, M., Talukder, M. S. U., Khan, M. H., Biswas, J. C., & Nemes, A. (2015). Validation of the AquaCrop model for irrigated rice production under varied water regimes in Bangladesh. In Agricultural Water Management (Vol. 159, pp. 331–340). Elsevier BV. https://doi.org/10.1016/j.agwat.2015.06.022

Maurer, E. P., & Hidalgo, H. G. (2008). Utility of daily vs. monthly large-scale climate data: an intercomparison of two statistical downscaling methods. In Hydrology and Earth System Sciences (Vol. 12, Issue 2, pp. 551–563). Copernicus GmbH. 10.5194/hess-12-551-2008

Meinshausen, M., Nicholls, Z. R. J., Lewis, J., Gidden, M. J., Vogel, E., Freund, M., Beyerle, U., Gessner, C., Nauels, A., Bauer, N., Canadell, J. G., Daniel, J. S., John, A., Krummel, P. B., Luderer, G., Meinshausen, N., Montzka, S. A., Rayner, P. J., Reimann, S., … Wang, R. H. J. (2020). The shared socio-economic pathway (SSP) greenhouse gas concentrations and their extensions to 2500. In Geoscientific Model Development (Vol. 13, Issue 8, pp. 3571–3605). Copernicus GmbH. 10.5194/gmd-13-3571-2020

Ministry of Agriculture, Forestry and Fisheries. (2022a). Annual report 2021 and Planning 2022.

Ministry of Agriculture, Forestry and Fisheries. (2022b). National Agricultural Development Policy 2022–2030.

Mirfenderski, R., Darzi-Naftchali, A., & Karandish, F. (2021). Climate-resilient agricultural water management to alleviate negative impacts of global warming in rice production systems. In Theoretical and Applied Climatology (Vol. 147, Issues 1–2, pp. 409–422). Springer Science and Business Media LLC. https://doi.org/10.1007/s00704-021-03813-8

Monaco, S., Volante, A., Orasen, G., Cochrane, N., Oliver, V., Price, A. H., Teh, Y. A., Martínez-Eixarch, M., Thomas, C., Courtois, B., & Valé, G. (2021). Effects of the application of a moderate alternate wetting and drying technique on the performance of different European varieties in Northern Italy rice system. In Field Crops Research (Vol. 270, p. 108220). Elsevier BV. https://doi.org/10.1016/j.fcr.2021.108220

Na, R., Vote, C., Oeurng, C., Song, L., & Lim, V. (2017). Predicting maize yield response to climate change: Case study in Cambodia. 2nd international symposium on conservation and Management of Tropical Lakes.

O'Neill, B. C., Tebaldi, C., van Vuuren, D. P., Eyring, V., Friedlingstein, P., Hurtt, G., Knutti, R., Kriegler, E., Lamarque, J.-F., Lowe, J., Meehl, G. A., Moss, R., Riahi, K., & Sanderson, B. M. (2016). The Scenario Model Intercomparison Project (ScenarioMIP) for CMIP6. In Geoscientific Model Development (Vol. 9, Issue 9, pp. 3461–3482). Copernicus GmbH. 10.5194/gmd-9-3461-2016

Oliver, V., Cochrane, N., Magnusson, J., Brachi, E., Monaco, S., Volante, A., Courtois, B., Vale, G., Price, A., & Teh, Y. A. (2019). Effects of water management and cultivar on carbon dynamics, plant productivity and biomass allocation in European rice systems. In Science of The Total Environment (Vol. 685, pp. 1139–1151). Elsevier BV. https://doi.org/10.1016/j.scitotenv.2019.06.110

Van Oort, P. A. J., & Dingkuhn, M. (2021). Feet in the water and hands on the keyboard: A critical retrospective of crop modelling at AfricaRice. In Field Crops Research (Vol. 263, p. 108074). Elsevier BV. https://doi.org/10.1016/j.fcr.2021.108074

Osman, R., Ata-Ul-Karim, S. T., Tahir, M. N., Ishaque, W., & Xu, M. (2022). Multi-model ensembles for assessing the impact of future climate change on rainfed wheat productivity under various cultivars and nitrogen levels. *European Journal of Agronomy, 139*, 126554. https://doi.org/10.1016/j.eja.2022.126554

Porras-Jorge, R., Ramos-Fernández, L., Ojeda-Bustamante, W., & Ontiveros-Capurata, R. (2020). Performance assessment of the AquaCrop model to estimate rice yields under alternate wetting and drying irrigation in the coast of Peru. In Scientia agropecuaria (Vol. 11, Issue 3, pp. 309–321). Universidad Nacional de Trujillo. https://doi.org/10.17268/sci.agropecu.2020.03.03

Raes, D., Steduto, P., Hsiao, TC., and Fereres, E. (2009). Crop water productivity. Calculation Procedures and Calibration Guideline. AquaCrop version 3.0. FAO. Land and Water Development Division, Rome.

Raes, D., Steduto, P., Hsiao, T.C., & Fereres, E. (2012). Reference manual of AquaCrop model. Chapter 2, Users Guide, FAO Land and Water Division, Rome Italy. 164p

Raes, D., Steduto, P., Hsiao, T, C., and Fereres, E. (2017). AquaCrop reference manual (Version 6.0). http://www.fao.org/land-water/databases-and-software/aquacrop/en/

(2021). Improved management may alleviate some but not all of the adverse effects of climate change on crop yields in smallholder farms in West Africa. In Agricultural and Forest Meteorology (Vols. 308–309, p. 108563). Elsevier BV. https://doi.org/10.1016/j.agrformet.2021.108563

Raoufi, R. S., & Soufizadeh, S. (2020). Simulation of the impacts of climate change on phenology, growth, and yield of various rice genotypes in humid sub-tropical environments using AquaCrop-Rice. *International Journal of Biometeorology, 64*(10), 1657–1673. https://doi.org/10.1007/s00484-020-01946-5

Raoufi, R. S., Soufizadeh, S., Larijani, B. A., AghaAlikhani, M., & Kambouzia, J. (2018). Simulation of growth and yield of various irrigated rice (Oryza sativa L.) genotypes by AquaCrop under different seedling ages. Natural

Resource Modeling, 31(2). https://doi.org/10.1111/nrm.12162

(2018). Methane emission reductions from the alternate wetting and drying of rice fields detected using the eddy covariance method. In Environmental Science & Technology (Vol. 53, Issue 2, pp. 671–681). American Chemical Society (ACS). https://doi.org/10.1021/acs.est.8b05535

Saito, K., Linquist, B., Atlin, G. N., Phanthaboon, K., Shiraiwa, T., & Horie, T. (2006). Response of traditional and improved upland rice cultivars to N and P fertilizer in northern Laos. *Field Crops Research, 96*, 216–223.

Sarwar, N., Atique-ur-Rehman, Ahmad, S., & Hasanuzzaman, M. (2022). Modern techniques of rice crop production. In Modern Techniques of Rice Crop Production. https://doi.org/10.1007/978-981-16-4955-4

Shi, P., Zhu, Y., Tang, L., Chen, J., Sun, T., Cao, W., & Tian, Y. (2016). Differential effects of temperature and duration of heat stress during anthesis and grain filling stages in rice. In Environmental and Experimental Botany (Vol. 132, pp. 28–41). Elsevier BV. https://doi.org/10.1016/j.envexpbot.2016.08.006

Shrestha, S., Deb, P., & Bui, T. T. T. (2014). Adaptation strategies for rice cultivation under climate change in Central Vietnam. In Mitigation and Adaptation Strategies for Global Change (Vol. 21, Issue 1, pp. 15–37). Springer Science and Business Media LLC. https://doi.org/10.1007/s11027-014-9567-2

Shrestha, M., Acharya, S. C., & Shrestha, P. K. (2017). Bias correction of climate models for hydrological modelling – are simple methods still useful? In Meteorological Applications (Vol. 24, Issue 3, pp. 531–539). Wiley. https://doi.org/10.1002/met.1655

Sokkea Hoy (2024) Grain and Feed Annual. USDA. Phnom Penh

Sriphirom, P., Chidthaisong, A., Yagi, K., Tripetchkul, S., & Towprayoon, S. (2019). Evaluation of biochar applications combined with alternate wetting and drying (AWD) water management in rice field as a methane mitigation option for farmers' adoption. In Soil Science and Plant Nutrition (Vol. 66, Issue 1, pp. 235–246). Informa UK Limited. https://doi.org/10.1080/00380768.2019.1706431

Steduto, P., Hsiao, T, C., Fereres, E., Raes, D. (2012). Crop yield response to water. FAO IRRIGATION AND DRAINAGE PAPER 66. FAO.

Thrasher, B., Maurer, E. P., McKellar, C., & Duffy, P. B. (2012). Technical note: Bias correcting climate model simulated daily temperature extremes with quantile mapping. In Hydrology and Earth System Sciences (Vol. 16, Issue 9, pp. 3309–3314). Copernicus GmbH. 10.5194/hess-16-3309-2012 H, Alghabari F, Huang J (2016) Exogenously applied plant growth regulators enhance the morpho-physiological growth and yield of rice under high temperature. Front Plant Sci 7:1250

Vahdati, A., Mohebalipour, N., Amiri, E., Ebadi, A. A., & Faramarzi, A. (2020). Simulating the production of rice genotypes by flood management and end-season water stress conditions using AquaCrop model. In Communications in Soil Science and Plant Analysis (Vol. 51, Issue 16, pp. 2137–2146). Informa UK Limited. https://doi.org/10.1080/00103624.2020.1813750

Xu, J., Bai, W., Li, Y., Wang, H., Yang, S., & Wei, Z. (2019). Modeling rice development and field water balance using AquaCrop model under drying-wetting cycle condition in eastern China. In Agricultural Water Management (Vol. 213, pp. 289–297). Elsevier BV. https://doi.org/10.1016/j.agwat.2018.10.028

Yao, F., Huang, J., Cui, K., Nie, L., Xiang, J., Liu, X., Wu, W., Chen, M., & Peng, S. (2012). Agronomic performance of high-yielding rice variety grown under alternate wetting and drying irrigation. In Field Crops Research (Vol. 126, pp. 16–22). Elsevier BV. https://doi.org/10.1016/j.fcr.2011.09.018

Zachow, M., Nóia, D. S., Júnior, R., & Asseng, S. (2023). Seasonal climate models for national wheat yield forecasts in Brazil. *Agricultural and Forest Meteorology, 342*, 109753. https://doi.org/10.1016/j.agrformet.2023.109753